A low frequency hybrid harvester with ring magnets

Article *in* Sustainable Energy Technologies and Assessments · February 2016

DOI: 10.1016/j.seta.2015.11.006

Sustainable Energy Technologies and Assessments 13 (2016) 23–30

Contents lists available at ScienceDirect

Sustainable Energy Technologies and Assessments

journal homepage: www.elsevier.com/locate/seta

Original Research Article

A low frequency hybrid harvester with ring magnets

Mohammed Salim [a,*], Jedol Dayou [b], Hakim S. Aljibori [c], Dhia Salim [d], Akeel Shebeeb [a]

[a] Universiti Tenaga, Mechanical Engineering Dept., Selangor, Malaysia
[b] Universiti Malaysia Sabah, School of Science and Technology, Jalan UMS, 88400 Kota Kinabalu, Sabah, Malaysia
[c] Mechanical Engineering, College of Applied Sciences, Ministry of Higher Education, Oman
[d] Ministry of Science and Technology, Baghdad, Iraq

ARTICLE INFO

Article history:
Received 23 November 2014
Revised 25 September 2015
Accepted 14 November 2015

Keywords:
Electromagnetic harvesters
Hybrid harvesters
MEMS
Ring magnets

ABSTRACT

Although many hybrid EH devices had been investigated by researchers, their performances at different operating resonance frequencies were not reported. Radial magnetic field was reported as the most efficient architecture to use in electromagnetic energy conversion, this was utilized in the design of a low frequency and efficient hybrid harvester comprising piezoelectric (PZT) and electromagnetic generators. FE simulation was used to obtain the magnetic field, design the coil and locate its position relative to the magnets. The electromagnetic generator consists of ring magnets which act as proof mass, with a hanging coil inside. The harvester was tested at frequency range of (34–40) Hz, produced maximum power of (710) μW. The maximum normalized power density and maximum efficiency of the harvester are (2.272) mW/cm^3/g^2 and (30.1%) respectively, at frequency of 36 Hz and induced acceleration of (0.25) g. The new hybrid harvester has a higher normalized power density compared with others.

Introduction

Piezoelectric and electromagnetic transducers are considered best suited to recover energy from mechanical vibrations [1]. The systems are used separately, but the combination of the two features multi functionality, and produces a hybrid generator. In the PZT generator, the proof mass may be used as part of an electromagnetic generator in addition to its function in tuning the frequency and enlarging the amplitude while the material of the suspending structure of an electromagnetic generator may be PZT, thus making additional use of it in producing power [2]. A vibration based generator produces maximum power at its resonant frequency which should match the ambient vibration frequency. Increasing the operation frequency range may be achieved through tuning or increasing the band width.

Wischke et al. [3] presented a double-side suspended hybrid generator with two magnets fixed at the middle of a PZT beam, to obtain more power from the magnets vertical movement, and conductors. The experimental tests covered different arrangements of magnets, inductors, and different interconnections of the bimorph layers with the conductors. The PZT and the electromagnetic generators produced (300) μW and (120) μW respectively, at resonant frequency of (753) Hz and acceleration of (10) m/s^2.

Khaligh et al. [4] built a mathematical model of the output power for a piezoelectric-electromagnetic hybrid power generation system by using an equivalent spring-mass-damping second-order vibration model, feasible to harvest energy from normal range of human activities for powering wearable electronic devices. The proposed design consists of a vibrating square disc connected to four PZT springs; the disc has a central hole with a copper coil placed inside and two permanent magnets fixed on top on opposite sides. Output powers of (37) mW and (6) mW for the electromagnetic and piezoelectric conversion parts respectively were expected from the proposed structure.

Karami and Inman [5] considered three coupling systems in building a unified mathematical model of a piezoelectric-electromagnetic hybrid harvester; the cantilever mechanical vibration system, the piezoelectric energy generator and the electromagnetic energy generator. Variations in excitation frequency and damping ratio effects were considered and a unified approximation method for a linear, softly nonlinear and bi-stable nonlinear energy harvester was established. Linear, nonlinear mono-stable and bi-stable hybrid energy harvesters were investigated as a case studies and the approximation method was found accurate.

* Corresponding author. Tel.: +60 1 492 92867.
E-mail address: engmdss@yahoo.com (M. Salim).

http://dx.doi.org/10.1016/j.seta.2015.11.006
2213-1388/

Challa et al. [6] presented a hybrid harvester consists of PZT and electromagnetic parts. To maximize the efficiency, the electrical damping induced by the energy harvesting mechanism was matched to the mechanical damping in the system by altering the effective magnetic field density through altering the relative displacement between the coil and the magnet. A maximum power of (332) μW at resonance frequency of (21.6) Hz was obtained and a power density of (9.5) μW/cm^3 was reported. A theoretical model was developed which agreed closely with the experimental results. Another device in the d_{33} mode was also tested, maximum power of (182) μW and power density of (3.2) μW/cm^3 were reported for the second device.

Yang et al. [7] reported a hybrid generator consists of a multi-layer piezoelectric cantilever, permanent magnets, and a substrate of two-layer coils. Different number of magnets and magnets locations were explored. The device produced maximum output power and voltage of (176) μW and (0.84) V respectively from the PZT part, and (0.19) μW, (0.78) mV for maximum output power and voltage respectively from the coils, under acceleration of (2.5)g and frequency of (310) Hz. Power densities of (790 and 0.85) μW/cm^3 were derived for the piezoelectric and electromagnetic sides respectively.

Beker et al. [8] proposed a hybrid harvester design for keyboards applications; it constitutes a PZT cantilever with a magnet proof mass and a planar coil. The dome structure under the keyboard was modified to support energy harvesting. A frequency-up-conversion technique was used in the design and a total power of (19.76) μW was expected. Wacharasindhu and Kwon [9] developed a micro-generator based on the piezoelectric and electromagnetic principles, and the mechanical energy from finger keystrokes. Maximum harvested powers of (40.8) μW with a (3) MΩ load from piezoelectric conversion and (1.15) μW with a (35) Ω load from electromagnetic conversion were obtained. An array build up possibility was claimed.

Shan et al. [10] presented a hybrid harvester comprising PZT bimorph and a magnetic levitation system consists of two outer disc magnets, fitted at the ends of a hollow cylindrical casing with a center magnet in between. The outer magnets repelled the center magnet. A spiral coil was wound around the casing at the center magnet level. The magnets, casing and the coil acted as a proof mass for the bimorph. At input acceleration of (5) m/s^2, the electromagnetic part produced maximum power of (8.46) mW at a frequency of 9 Hz whereas the PZT part produced maximum power of (19.9) m W at resonance frequency of (16) Hz.

Shan et al. [11] reported a new mathematical model for a piezoelectric electromagnetic hybrid energy harvester comprises two vibrating square magnets with a stationary coil in between. The experiments produced a peak output power of (4.25) mW for the hybrid harvester; it represented an increase of (13.3%) over the single piezoelectric harvester. Experiments results verified the numerical analysis. Values of efficiencies, induced acceleration and power densities were not reported.

A multimodal hybrid harvester was presented by Tadesse et al. [12]; the device consists of six piezoelectric plates bonded on both sides of a trapezoidal cantilever at maximum stress locations. Trapezoidal shape produces more uniform strain distribution along the cantilever length. An attached permanent magnet at the tip of the cantilever acted as proof mass in addition of being part of the electromagnetic generator. The harvester was tested at its first and second modes of (20, 300) Hz with induced acceleration of (35)g. The prototype produced powers of (0.25) W from the electromagnetic mechanism and (0.25) mW from the piezoelectric mechanism at resonant frequency of (20) Hz. The calculated volumes of the electromagnetic system and the piezoelectric system were (8.3106 and 3.6231) cm^3 respectively. The harvester produced negligible or no power at acceleration below (5)g according to the performance curves.

Two degrees of freedom (TDOF) based hybrid harvester was introduced by Wang et al. [13]. A mathematical model based on the second order differential equation of motion and equivalent electrical circuits was derived and used to investigate the effect of the effective electromechanical coupling coefficients (for the PZT and the electromagnetic generators) on the maximal power outputs from various harvester configurations. Two piezoelectric elements bonded symmetrically to a brass clamped beam constitute the PZT generator. The electromagnetic generator consists of a spring, a magnet, and a cylindrical coil. The hybrid harvester was tested with induced acceleration of (0.1)g, in a frequency range of (65–95) Hz, produced two peaks and maximum power output (2.16) mW compared with (1.68 and 0.96) mW from the TDOF stand-alone electromagnetic and PZT generators respectively.

A comparison of different electrodynamics transducer architectures using numerical simulations was performed to find the most efficient magnetic field orientation, the study concluded that an opposing magnet architecture which produces radial magnetic field in the gap between the magnets has the highest transduction coefficient [14]. Our previous work [15] took this into consideration and introduced the ring magnet hybrid energy harvester. This paper is a continuation where finite element (FE) was employed in obtaining the ring magnets characteristics and designing a coil for the electromagnetic part of the hybrid harvester accordingly.

Theory

Williams and Yates [16] developed a generic model based on inertial kinetic energy for power calculation of energy harvesters. The model considers a forced vibration lumped mass second order dynamic system. The instantaneous dissipated power (P) within the damper for a sinusoidal vibration signal equals the product of the velocity and the damping force. Eq. (1) was derived and used to compute the maximum output power.

$$P_{emax} = \frac{ma^2}{16\zeta_m \omega_n} \tag{1}$$

where (P_{emax}) is the maximum electrical power that can be extracted from the system, (m) is the vibrating mass, (ζ_m) is the mechanical damping ratio and (ω_n) is the system resonant frequency.

The mechanical damping ratio can be determined using Eq. (2) for logarithmic decay

$$\zeta_m = \frac{\ln\left(\frac{a_1}{a_2}\right)}{2\pi n} \tag{2}$$

where (a_1, a_2 and n) represent the amplitudes of the first cycle, the last cycle and the number of cycles considered respectively.

In energy harvesters, the electrodynamics transduction coefficient (K) or what is sometimes called the coupling coefficient is an important parameter which affects the degree of transformation of mechanical energy to electrical energy. Cheng et al. [17] used the coupling coefficient in rewriting Eq. (1) for electromagnetic generators as

$$P_{emax} = \frac{(ma)^2}{8b} \times \frac{1}{\left(\frac{R_{coil} b}{K^2}\right) + 1} \tag{3}$$

where (b and R_{coil}) are the damping coefficient and the coil resistance of the generator (Ω).

For a coil crossing radial magnetic field, a parameter named coupling strength (γ) was introduced which is given by

$$\gamma = \frac{K^2}{R_{coil} b} = \frac{\left(\int B_{rad}\, dl\right)^2}{\rho \frac{l_{coil}}{A_{coil}} b}$$

$$\gamma = \frac{(B_{rad})^2 V_{coil}}{\rho b} \tag{4}$$

where (V_{coil}, A_{coil}, l, B_{rad} and ρ) are the coil material volume (m^3), the wire cross sectional area (m^2), the conductor length (m), the average radial flux density over the conductor volume (T), and the coil wire resistivity (Ωm) respectively.

$$\text{The theoretical power ratio} = \frac{\text{Power obtained from Eq. (3)}}{\text{Power obtained from Eq. (1)}}$$

$$= \frac{\frac{(ma)^2}{8b} \times \frac{1}{\left(\frac{R_{coilb}}{K^2}\right)+1}}{\frac{ma^2}{16\zeta_m \omega_n}} = \frac{2m\zeta_m\omega_n}{b\left(\frac{bR_{coil}}{K^2}+1\right)} \tag{5}$$

$$= \frac{2m\zeta_m\omega_n}{b\left(\frac{1}{\gamma}+1\right)} = \frac{1}{\left(\frac{1}{\gamma}+1\right)}$$

Fig. 1 shows the theoretical variation of the power ratio with the coupling strength. Theoretically, in order to achieve a power ratio >90%, the coupling strength needs to be greater than (10).

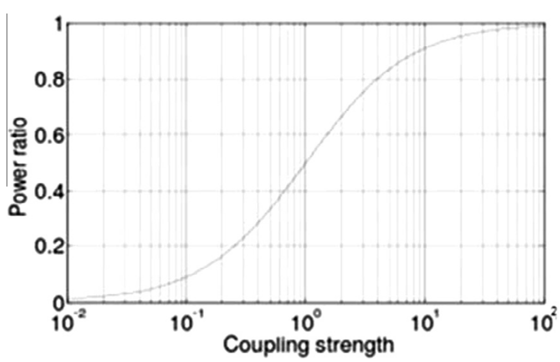

Fig. 1. Theoretical relationship between the power ratio and the coupling strength for electromagnetic generator subjected to radial magnetic field.

Methodology

For additional harvesting, a commercial brass reinforced PZT bimorph type PSI-5H4E with opposite polling was used as the cantilever for the PZT generator part of the hybrid harvester. The cantilever length, width, PZT layer thickness and brass thickness were (25, 12.7, 0.190, and 0.130) mm respectively. Table 1 shows the properties of a single sheet of the mentioned PZT material which was obtained from the manufacturer, Piezo System Inc.

The proof mass consists of NdFeB ring magnets with ID × OD × height of (10, 20, and 3.5) mm respectively, weighs (6) g each, and drilled steel shims with dimensions of (12.7 × 6.5) mm of different thicknesses, held together by screw and nut. The ring magnets are mounted on a seat at the tip, on the top side of the cantilever. The seat concentrates the magnets weights at the tip. The steel shims are fixed at the tip, on the bottom side of the cantilever. Tuning may be achieved by two means, either altering the number of magnets or the total steel shims mass but only the later was considered as altering the number of magnets should be accompanied by a different coil and coil location.

The magnetic field densities and directions of the employed ring magnets were obtained from simulation using Maxwell Ansoft SV software; this led to design the copper wire coil and its location with respect to the ring magnets. The copper coil was wound round a (6) mm PTFE screw and then hanged inside the magnets, resulted in the completion of the hybrid harvester assembly. Fig. 2 is a schematic diagram of the harvester; Fig. 3(a) shows the mounted harvester assembly with the coil hanging partly inside the magnets and (b) illustrates the shims assembly.

The instruments consist of a shaker type Lab Work ET-132-2 where the cantilever structure was mounted. The frequency and acceleration of the shaker were controlled by a frequency sweeper and control system type (Labview) of National Instruments (NI) make. The system includes the electronic cards (NI PXI-4482) for vibration monitoring and control, (NI PXI-5421) for controlling the shaker performance via the amplifier and (NI PXI-4072) for continuous monitoring and recording of the PZT generator output voltage. An accelerometer was attached to the cantilever mounting structure to measure the frequency, acceleration and provides feedback to the control system. A multimeter was used for voltage measurements across the coil. The cantilever surfaces at the fixed end were connected through wires to the Labview system to record the output voltage. Fig. 4 represents the instruments block wiring diagram.

Table 1
Piezoelectric and material properties of PSI-5H4E single sheet.

Piezo systems designation	5H4E (industry type 5H, navy type VI)			
Composition	Lead zirconate titanate			
Property		Symbol		Units
Piezoelectric	Relative dielectric constant (@ 1KHz)	K_3^T	3800	
	Piezoelectric strain coefficient	d_{33}	650×10^{-12}	m/V
		d_{31}	-320×10^{-12}	
	Piezoelectric voltage coefficient	g_{33}	19×10^{-3}	Vm/N
		g_{31}	-9.5×10^{-3}	
	Coupling coefficient	K_{33}	0.75	
		K_{31}	0.44	
	Polarization field	E_P	1.5×10^6	V/m
	Initial Depolarization field	E_c	3×10^6	V/m
Mechanical	Density	ρ	7800	kg/m^3
	Mechanical Q		32	
	Elastic modulus	Y_3^E	5×10^{10}	N/m^2
		Y_1^E	6.2×10^{10}	
Thermal	Thermal expansion coefficient		3×10^{-4}	m/m °C
	Curie temperature		230	°C

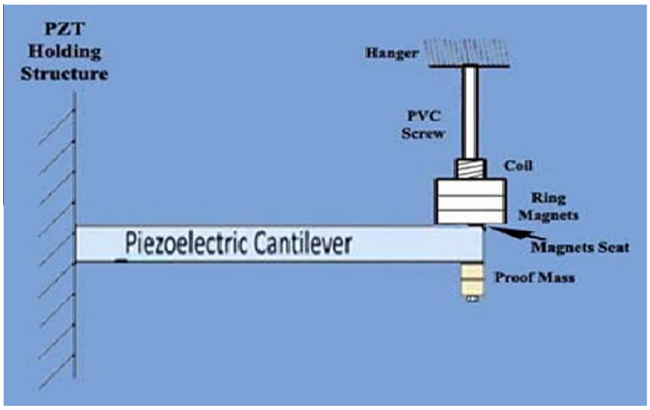

Fig. 2. Schematic diagram of the hybrid harvester.

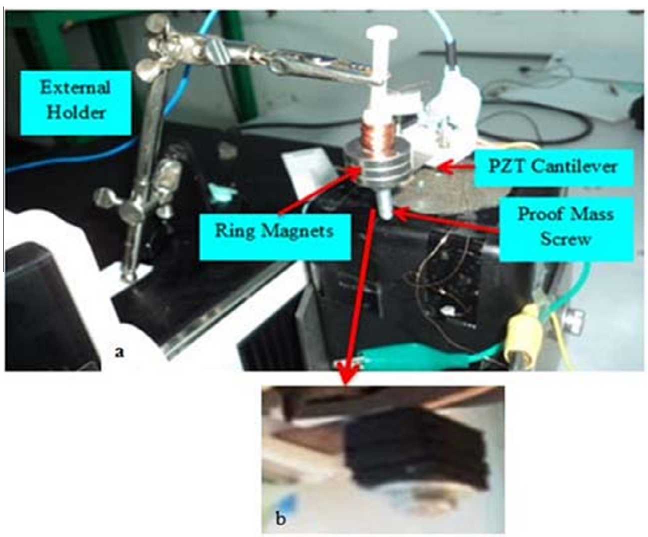

Fig. 3. (a) The hybrid harvester mounted on the shaker, (b) the proof mass assembly.

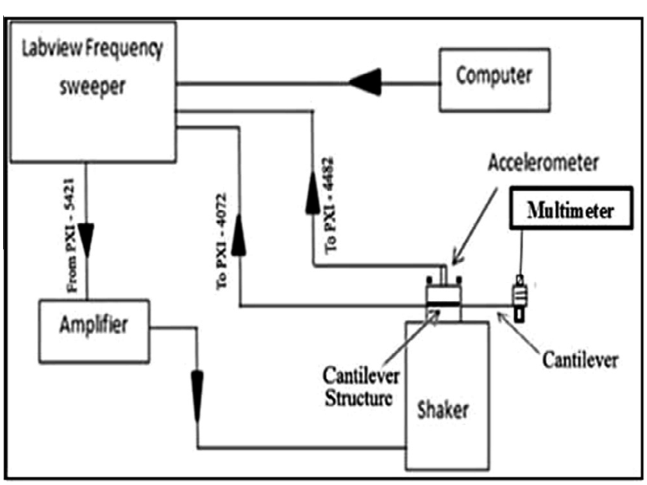

Fig. 4. Block diagram of the instruments wiring.

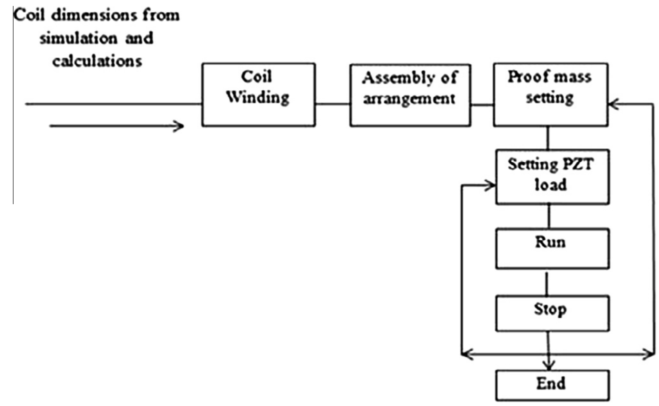

Fig. 5. Flow chart for the hybrid experiments.

The frequency sweeper possesses settings for starting frequency and stopping frequency, these settings were adjusted accordingly prior to the start of each run. Settings of acceleration, margin, frequency step, amplitude step, wait after amplitude change and wait before measurements were adjusted to (0.25g, 0.02g, 1 Hz, 0.002 V, 2 s, 5 s) respectively and remained unchanged for all runs.

Prior to the harvester test runs, and in order to calculate the mechanical damping ratio (ζ_m), the PZT cantilever leads were connected to a digital storage oscilloscope type GDS-820/GDS-840 of GOOD WILL Instrument Co., Ltd. The PZT cantilever was set in vibration at different resonance frequencies, each time the output voltage signal was observed on the oscilloscope, subsequently the shaker was switched off and the attenuated signal was recorded. Eq. (2) was used for (ζ_m) evaluation.

A series of runs were conducted for a range of proof mass (18–24) g, increasing or reducing the shims and the number of magnets controls the total proof mass value and hence the resonant frequency. For each resonant frequency, various resistances were applied across the PZT cantilever, the corresponding voltages obtained were recorded by the labview and the corresponding output power was calculated in order to find the optimum power at that frequency. For each of the PZT optimum power runs, the reading of the voltage across the coil of the electromagnetic generator was recorded from the Multimeter. Fig. 5 is a flow chart of the experimental procedure.

In order to find the optimum useful power of the electromagnetic generator at frequency of 36 Hz where maximum PZT power was produced, various resistances were applied across the coil and the corresponding voltages were recorded from the Multimeter.

All experimental readings obtained, theoretical and experimental calculations were tabulated and corresponding graphs were plotted.

Results and discussions

This section shows the results, calculations and discussions for:

- FE Simulation for the ring magnets and coil design
- The hybrid harvester theoretical and experimental performance

FE simulation for ring magnets and coil design

Maxwell Ansoft was used to design the electromagnetic generator part; Fig. 6 is a vertical cross section picture of the magnetic flux magnitudes and directions obtained from simulation for three of the specified axially magnetized ring magnet. The figure shows that the directions of the radial field or the field radial components in the upper half are inwards and opposite to that in the lower half which are outwards, this means that the magnetic fields in the two halves induce opposite effects and this is why the coil location is restricted to the magnetic field with inwards direction in the top

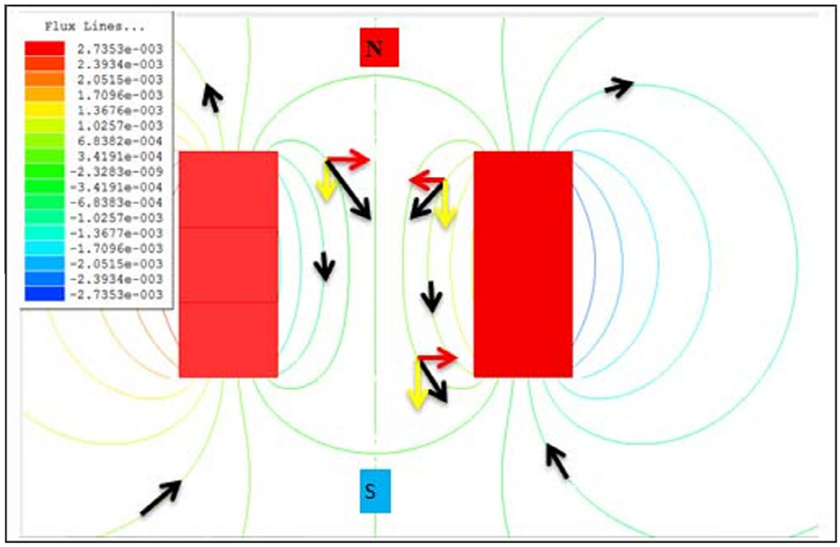

Fig. 6. Magnetic flux magnitudes and directions of the used three ring magnets.

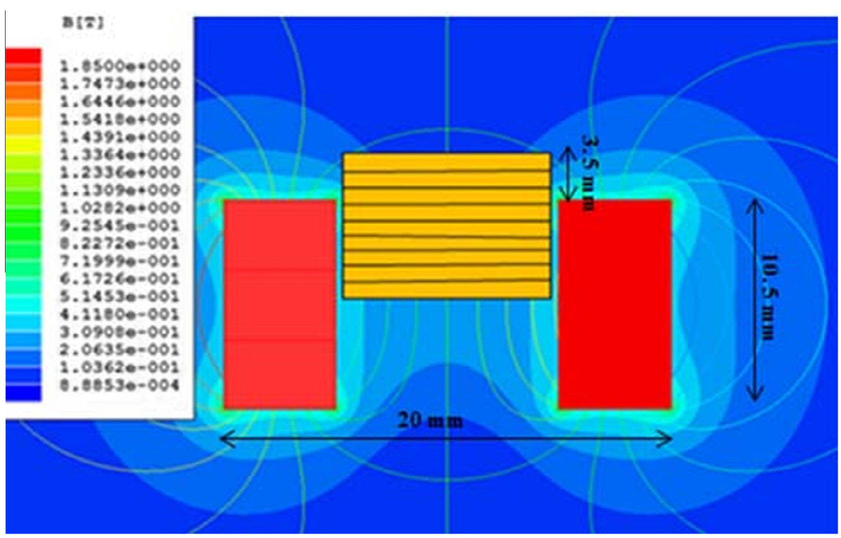

Fig. 7. Magnetic field of the three axially magnetized rings and the relative coil position.

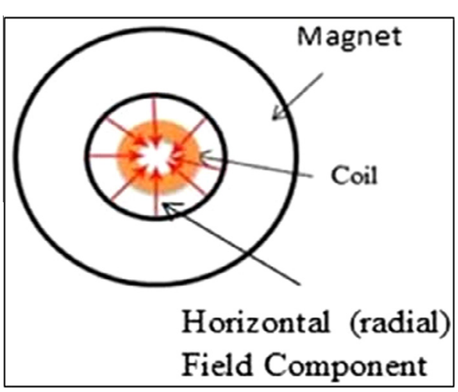

Fig. 8. A cross sectional sketch of the electromagnetic generator.

half, i.e. size and location of the coil are governed by the field radial components.

Fig. 7 indicates the flux directions and the magnetic field densities around, and inside the magnets. It shows a field strength of 0.35 Tesla near the two end surfaces and close to the inside surface. Fig. 7 was used to define the space and location of the coil according to the effective field radial components of the same orientation. A copper wire coil of (9.7, 6, 8) mm as outside diameter × inside diameter × thickness respectively was considered. A copper wire of (0.15) mm in diameter was used to wind a coil of volume (183) mm^3, average number of turns (427) and measured resistance of (10) Ω, assuming filling factor of (0.5). The coil was then suspended partly inside the magnets with (3.5) mm outside. Fig. 8 is a cross section illustrates the considered radial field with respect to the coil and magnets; the movement of the magnet is perpendicular to the paper.

Eq. (5) shows that the theoretical power ratio is a function of the coupling strength (γ) and hence the radial magnetic flux density (B_{rad}). Ring magnets of similar dimensions but of different magnetic orientations (diametrically magnetized and radially magnetized) were simulated; the magnetic flux directions of the first were not suitable while the flux density of the second was higher than the axially magnetized magnet, but overloaded the harvester.

Hybrid harvester theoretical and experimental performance

The mechanical damping ratio (ζ_m) was calculated by substituting the values of amplitudes obtained from the oscilloscope in Eq. (2), the calculated average value for the mechanical damping ratio was (0.05). Values of (b) were calculated using (1.1×10^3) N/m for beam stiffness and the different values of proof mass (m). Eq. (4) was used to calculate (γ) by substituting the values of 0.25 T for B_{radial} as the mean value from simulation, $\rho = 1.68 \times 10^{-8}$ Ωm and the corresponding values of (b). Corresponding theoretical power ratios were then obtained from Fig. 1.

The experimental output power of the electromagnetic generator (P_{em}) is given by

$$P_{em} = \frac{V_{em}^2}{R_{coil} + R_{load}} \tag{6}$$

where V_{em} and R_{load} represent the output voltage and the load resistance respectively.

Assuming that R_{coil} is dominating at low frequencies, it is the only load and equal (10) Ω as it was measured, the corresponding electromagnetic generator optimum powers were calculated.

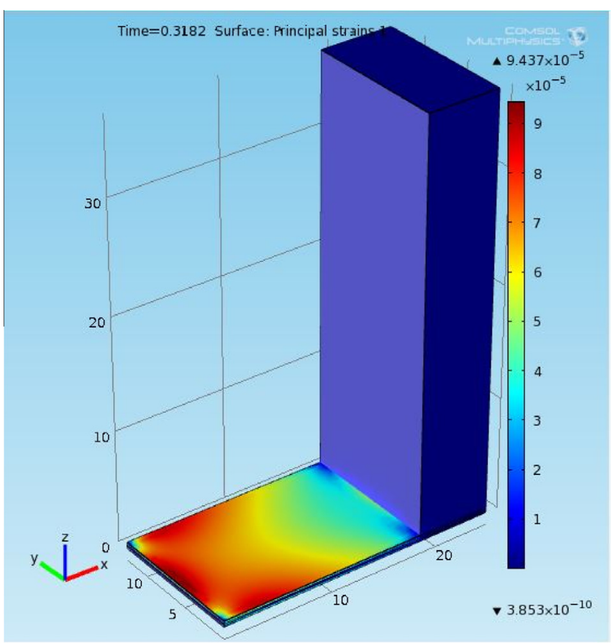

Fig. 9. Snapshot showing the strain distribution of the vibrating cantilever at maximum deflection using Comsol software.

$$\text{The experimental power ratio} = \frac{P_{em}}{\text{Power obtained from Eq. (1)}} = \frac{\frac{V_{em}^2}{R_{coil}+R_{load}}}{\frac{ma^2}{16\zeta_m\omega_n}} = \frac{16V_{em}^2\zeta_m\omega_n}{ma^2(R_{coil}+R_{load})} \tag{7}$$

Eq. (7) shows that the resonance frequency and the proof mass are factors in the equation within the allowed PZT strain limit, so Comsol multiphysics software was used to predict the resonance frequencies of the cantilever for different proof mass first and the resulted strain later. Fig. 9 is a snapshot showing the strain distribution along the bimorph cantilever as part of the carried out research.

Table 2 shows the theoretical and experimental performance of the hybrid generator.

Where V_{PZT}, P_{PZT}, P_{hyb}, P_{emax} and η_{PZT} represent the output voltage of the loaded PZT generator, the PZT generator power output, the total hybrid harvester power output, the maximum power that can be extracted from the PZT vibrating cantilever and the efficiency of the PZT generator respectively.

Table 2 shows that, for the electromagnetic generator, the theoretical power ratios compare favorably with the experimental values apart from the low experimental value at (34) Hz which is due to the coil cutting weaker magnetic field. For the PZT generator, Fig. 10 represents the variations of the maximum output power and the corresponding voltage at different resonant frequencies (P_{PZT}, V_{PZT}) versus load resistance; it shows maximum output power of (0.3) mW and voltage of (9.5) V corresponding to resistance of (300) KΩ. For comparison, plots of the power variations of all generators with resonant frequency are shown in Fig. 11.

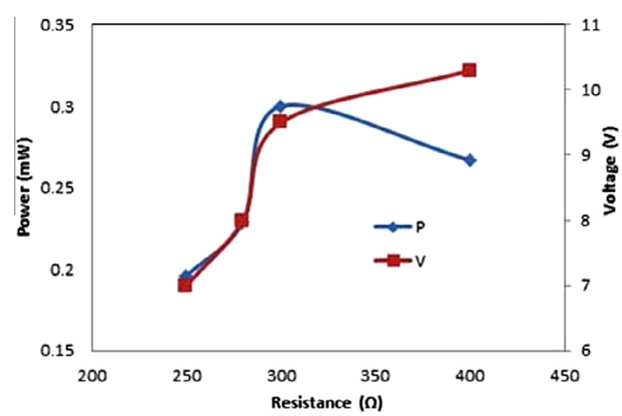

Fig. 10. Variations of power (P_{PZT}) and voltage (V_{PZT}) versus resistance for the PZT generator.

Table 2
Performance of the hybrid generator.

Proof mass (g)	Resonant frequency (Hz)	V_{em} (mV)	P_{em} (mW)	V_{PZT} (V)	Load resistance PZT (KΩ)	P_{PZT} (mW)	P_{hyb} (mW)	P_{emax} (mW)
18	40	57	0.325	7.0	250	0.196	0.521	0.534
20	38	61	0.372	8	280	0.232	0.604	0.625
22	36	64	0.410	9.5	300	0.300	0.710	0.725
24	34	44.5	0.224	10.3	400	0.267	0.491	0.838

Frequency (Hz)	Exp. power ratio $\left(\frac{P_{em}}{P_{emax}}\right)$	Theoretical power ratio	$\eta_{PZT}\left(\frac{P_{PZT}}{P_{emax}}\right)\%$
40	0.608	0.62	36.7
38	0.595	0.59	37.1
36	0.565	0.56	41.3
34	0.267	0.54	31.9

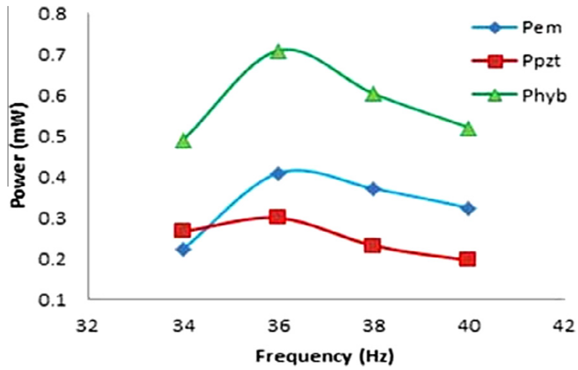

Fig. 11. Power versus frequency for the hybrid harvester and their components.

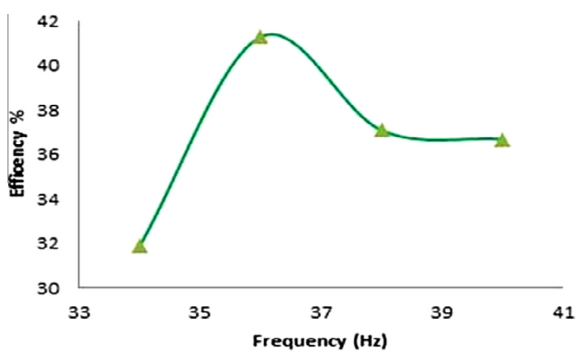

Fig. 12. Efficiency versus frequency for the PZT generator.

Fig. 12 shows the variations of efficiency with resonance frequency for the PZT generator, it shows maximum efficiency of 41.3% at 36 Hz. The calculations were based on the mechanical power available for conversion (P_{emax}).

It was unable to calculate the optimum useful power across the electromagnetic generator, but this is simply obtained from the voltage division between load resistance and coil impedance as the maximum power will be transferred to the load when the load and coil impedance are equal [18].

$$P_{emax} = \frac{(32)^2}{10} = 0.103 \text{ mW at } 36 \text{ Hz}$$

The hybrid maximum efficiency η_{hyb} at 36 Hz is given by

$$\eta_{hyb} = \left(\frac{P_{hyb}}{2P_{emax}}\right) = 27.8\%$$

The total volume of the two ring magnets, the coil upper part, the lower proof mass of (10 g) and the cantilever is 5.001 cm^3; this leads to normalized power density of (2.272) mW/cm^3/g^2 at resonant frequency of (36) Hz.

Conclusions

Different energy sources scale differently, so different bench points need to be used for comparisons depending on the focus of research [19]. The research was focused on resonating hybrid harvesters, and although Cebnik and Wallrabe [19] study was confined to electromagnetic vibration energy harvesters, the power, volume, frequency and acceleration were used as benchmark parameters for most comparisons, Table 3 was constructed accordingly for comparison of the reported resonating hybrid harvesters. It shows that only three of the references reported the power densities. Judging by the reported values for magnet weight, cantilever weight, proof mass, spring coil volume and the estimated total space the device occupies, the TDOF harvester presented by Wang et al. [13] seems to be not competitive in normalized power density, so the presented hybrid harvester has higher normalized power density than the reported others. The use of ring magnets proved to be an efficient way for energy conversion. Radially magnetized ring magnets have higher magnetic field densities than axially magnetized and hence produce more power but they are more difficult to manufacture. Coil wire radius affects the output voltage and power, thinner wire produces high voltage while thicker wire produces higher power.

Increasing or decreasing the proof mass was simple; it means tuning of the harvester was simply achieved and may be carried out in situ. Reducing the number of ring magnets and using shorter coil allow further tuning for higher frequencies.

The presented hybrid harvester is competitive for having high normalized power density and it is operated at low acceleration.

The induced vibration acceleration used during theoretical calculations and experimental work is 0.25g; this is an acceptable value for large rotating machines operating within the tested frequencies like AC motors, gear boxes, fans, pumps and centrifuges. This indicates that the designed hybrid generator can be utilized in industry unlike the others which require higher not acceptable acceleration. Employing the power produced from the electromagnetic part of the hybrid harvester in designing a hybrid harvester with synchronized switch harvesting on inductor (SSHI) system is recommended for future work as reported by Becker et al. [20].

Acknowledgments

The support of the Mechanical Engineering Department of Universiti Tenaga Nasional in Malaysia is greatly acknowledged,

Table 3
Comparison of different reported hybrid harvesters.

Researchers	Freq. (Hz)	Acc. (g)	Generators powers (mW)	Normalized power density (mW/cm^3/g^2)
Wischke et al. [3]	753	1	0.3 (total)	
Khaligh et al. [4]	–	–	6 (PZT), 37(em.)	
Challa et al. [6]	21.6	–	0.332 (total)	0.0095 (mW/cm^3)
Yang et al. [7]	310	2.5	0.176 (PZT), 0.00019 (em.)	0.126
Beker et al. [8]	–	–	0.01976	
Wacharasindhu and Kwon [9]	–	–	0.041 (PZT), 0.00115 (em.)	
Shan et al. [10]	16 (PZT), 9 (elec.)	0.51	19.9 (PZT), 8.46 (em.)	
Shan et al. [11]	–	–	4.25 (total)	
Tadesse et al. [12]	20, 300	35	0.25 (PZT), 250 (em.) at 20 Hz	0.017
Wang et al. [13] (TDOF system)	65–95	1	2.16 (total)	
Salim et al. [15]	36	0.25	0.300 (PZT), 0.410 (em.)	2.272

Assoc. Prof. Hanim Salleh in particular. This research was partially funded by Tenaga National Berhad Malaysia through Universiti Tenaga Nasional.

References

[1] Roundy S, Wright PK, Rabaey JM. Energy scavenging for wireless sensor networks. Norwell: Kluwer Academic Publisher; 2003.
[2] Wischke M, Woias P. A multi-functional cantilever for energy scavenging from vibrations. In: Proceedings of power MEMS; 2008. p. 73–6.
[3] Wischke M, Masur M, Woias P. A hybrid generator for vibration energy harvesting applications. In: Solid-state sensors, actuators and microsystems conference, transducers international; 2009. p. 521–24.
[4] Khaligh A, Zeng P, Wu X, Xu Y. A hybrid energy scavenging topology for human-powered mobile electronics. In: Industrial electronics, IECON 34th annual conference of IEEE; 2008. p. 448–53.
[5] Karami AM, Inman JD. Equivalent damping and frequency change for linear and nonlinear hybrid vibrational energy harvesting systems. J Sound Vibr 2011;330:5583–97.
[6] Challa V, Prasad MG, Fisher TF. A coupled piezoelectric–electromagnetic energy harvesting technique for achieving increased power output through damping matching. Smart Mater Struct 2009;18:095029.
[7] Yang BKW, Lim PS, Lee C. Hybrid energy harvester based on piezoelectric and electromagnetic mechanisms. J Micro/Nanolithogr MEMS MOEMS 2010;9:023002.
[8] Beker L, Zorlu O, Kulah K, Muhtaroglu A. Hybrid energy harvesting from keyboard. In: IEEE energy aware computing on (ICEAC); 2011. p. 1–4.
[9] Wacharasindhu T, Kwon WJ. A micromachined energy harvester from a keyboard using combined electromagnetic and piezoelectric conversion. J Micromech Microeng 2008;18:104016.
[10] Shan X, Guan S, Liu Z, Xu Z, Xie T. A new energy harvester using a piezoelectric and suspension electromagnetic mechanism. J Zhejiang Univ Sci A 2013;14:890–7.
[11] Shan X, Xu Z, Song R, Xie T. A new mathematical model for a piezoelectric-electromagnetic hybrid energy harvester. Ferroelectrics 2013;450:57–65.
[12] Tadesse Y, Zhang S, Priya S. Multimodal energy harvesting system: piezoelectric and electromagnetic. J Intell Mater Syst Struct 2009;20.
[13] Wang H, Tang L, Guo Y, Shan X, Xie T. A 2DOF hybrid energy harvester based on combined piezoelectric and electromagnetic conversion mechanisms. J Zhejiang Univ Sci A 2014;15(9):711–22.
[14] Spreemann D, Folkmer B, Manoli Y. Comparative study of electromagnetic coupling architectures for vibration energy harvesting devices. In: Tech. dig. 8th int. workshop on micro and nanotechnology for power generation and energy conversion apps; 2008. p. 257–60.
[15] Salim MD, Salleh H, Salim DS. A low frequency tunable hybrid generator. Microsyst Technol 2013;19:1839–44.
[16] Williams BC, Yates BR. Analysis of a micro-electric generator for microsystems. Sens Actuators A 1996;52:8–11.
[17] Cheng S, Natarajan DR, Arnold PD. The importance of coupling strength for maximizing the output power of electrodynamic vibrational energy harvesters. Proc Power MEMS 2010:351–4.
[18] Saha CR, O'Donnell T, Loder H, Beeby S, Tudor J. Optimization of an electromagnetic energy harvesting device. IEEE Trans Magn 2006;42(10):3509–11.
[19] Cepnik C, Wallrabe U. On the comparison, scaling and bench mark in electromagnetic vibration energy harvesters. Power MEMS 2011.
[20] Becker P, Folkmer B, Manoli Y. The hybrid vibration generator, a new approach for a high efficiency energy scavenger. In: Power MEMS. Washington DC, USA; 2009.